HHS Public Access

Author manuscript

RSC Adv. Author manuscript; available in PMC 2015 June 30.

Published in final edited form as:

RSC Adv. 2015 ; 5(48): 38117–38124. doi:10.1039/C4RA16803H.

Proliferation of preosteoblasts on TiO_2 nanotubes is FAK/RhoA related

He Zhang[a,‡], **Sheng Yang**[a,‡], **Nagasawa Masako**[b,c], **Dong Joon Lee**[c], **Lyndon F. Cooper**[c,d,*], and **Ching-Chang Ko**[c,e,*]

[a]Chongqing Key Laboratory of Oral Diseases and Biomedical Sciences, Chongqing Municipal Key Laboratory of Oral Biomedical Engineering of Hi gher Education, College of Stomatology, Chongqing Medical University, Chongqing 401147, China

[b]Division of Bioprosthodontics, Department of Oral Science, Niigata University Graduate School of Medical and Dental Sciences, Niigata 951-8514, Japan

[c]NC Oral Health Institute, School of Dentistry, University of North Carolina, CB #7454, Chapel Hill, NC 27599, USA

[d]Department of Prosthodontics, School of Dentistry, University of North Carolina, CB #7450, Chapel Hill, NC 27599-7450, USA

[e]Department of Orthodontics, School of Dentistry, University of North Carolina, CB #7450, Chapel Hill, NC 27599-7450, USA

Abstract

Topographies promote surface-dependent behaviors which may positively influence peri-implant bone healing. In this study the topological effects of TiO_2 nanotubes (TNTs) on aspects of preosteoblast behavior was investigated. Specifically, we hypothesize that TNTs can influence cell proliferation of preosteoblasts through cell adhesion and related modulation of FAK and RhoA. By culturing MC3T3-E1 cells on TNTs with different diameters (40nm and 150nm diameters), topography-dependent modulation in cell morphology and cell growth were observed. The average spreading area of the cell on Flat Ti, 40nm TNTs and 150nm TNTs were respectively 2176.05 μm^2, 1510.44 μm^2 and 800.72 μm^2. Proliferation increased among cells cultured on the 150nm TNTs (28.6%) compared with on Flat Ti (17.06%). The expression of FAK was 86.2% down regulated superimposition of TNTs topography. RhoA expression only slightly decreased (45.9%). Increasing TNT diameter enhanced initial adherent cell growth, which was relevant to the increased RhoA-to-FAK ratio in the cell. Increased TNT diameter was associated with higher ratio and greater proliferation in the first 24 hours. These findings not only support our hypothesis, but suggest that RhoA might be critically involved in TNTs mediated cell proliferation. Future investigation using functional gain and loss of RhoA may further reveal its mechanism.

Abstract

*Corresponding author: Tel: (+001) 919-537-3191, Ching-Chang_Ko@unc.edu, Lyndon_Cooper@unc.edu.
‡Both authors contributed equally to this work.

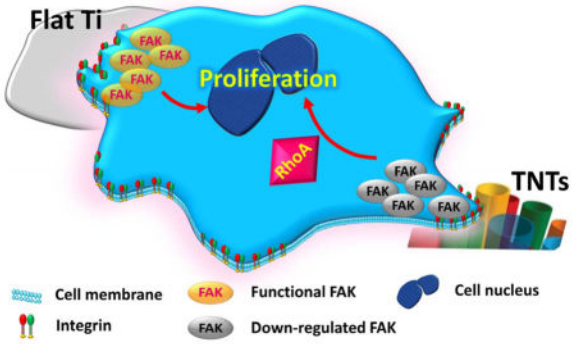

Model for FAK-RhoA modulation of topography-regulated proliferation.

1. Introduction

The increased concern about the interaction between implant surfaces and osteoblasts has led the research on implant surface topography cues to new areas. The ideal implant surface should not only promote early adhesion of osteoblasts, but more importantly, should also facilitate cell proliferation, which subsequently helps provide the precondition for bone formation. The creation of a material that can meet all these conditions is challenging. Compared with micro and macro-topography, surfaces with a more defined, reliable and reproducible nanostructure roughness provide a more conducive environment for osteoblast function in vivo.[1] Due to the advantageous high surface-to-volume ratio as well as higher degree of biocompatibility, titanium dioxide nanotubes (TNTs) are of particular interest.[2,3] Cell activity is directed by cell-implant surface interactions and a series of subsequent intracellular cascades would be triggered by the material topography.[4] The response of preosteolasts to TNTs has been mainly reflected in different cell behaviors, such as adhesion, morphology, proliferation, migration, survival, and differentiation.[5] Recently, it has been found that 70–100nm diameter TNTs might control the degrees of cell adhesion.[6–8] However, the related information about how they affect bioactivities of cells still remains lacking.

The interaction between cells and an inert substrate (no chemical leaching) is initiated by the formation of focal adhesion (FA), which leads to sequential arrangement of the actin cytoskeleton as well as mechanotransduction within the cells. These cellular cascades yield varied levels of gene and protein expression that contribute to activating or deactivating related signal pathways.[4] Focal adhesion kinase (FAK) - a cytoplasmic tyrosine kinase which localizes in focal contacts - is an essential mediator in ECM/integrin signaling transduction pathways.[9,10] FAK-dependent pathways have been associated with cell survival and cell cycle[11]. The influential role of FAK in cell proliferation has been reported in numerous studies.[12–14] Overexpressed FAK is thought to enhance the transcriptional activities of cyclin D1 (cell cycle regulator).[15] Nevertheless, the expression of FAK is not necessarily required for cell proliferation since FAK RNAi treated cells and FAK−/− cells both showed notable proliferation rates.[16] Hence, the modulatory role of FAK in ECM/integrin-regulated proliferation appears to be bifunctional, and depends on other molecular signaling pathways that modulate the formation of focal adhesion complex.[13]

RhoA functions downstream of integrin signaling and directs the realignment of cells under mechanical stretch-induced stimuli by reorganization of cytoskeleton.[17] Meanwhile, it is noteworthy that RhoA and its downstream effector Rho-associated kinase (ROCK) has been shown to contribute to mediating cell growth regulation at the level of cell-cycle machinery in terms of signal transduction, say promoting role in cell cycle progression.[18,19] While FAK and RhoA both can affect cell proliferation, the complementary relationship between them was proposed by an earlier biological study.[13] Sequentially, whether the same phenomenon could be traced by biophysical stimuli (e.g., nanotopography) to induce cell proliferation, and whether there is proportional relation existing between the expression of FAK and RhoA has not been explored.

2. Materials and methods

To test our hypothesis whether TNTs affect the proliferation of preosteoblasts associated with FAK/RhoA, all experiments were carried out on Flat Ti as control group, and 40nm TNTs or 150nm TNTs fabricated using two different voltages respectively. For outcome assessment, we investigated the adherent cell morphology, cell proliferation, and the protein expression of FAK, pY397-FAK and RhoA. The relative level of RhoA to FAK was measured by densitometry analysis of the immunoblots. To determine the effects of pY397-FAK and RhoA on cell growth, FAK Y397 and RhoA inhibitors were applied to cultured cells. The osteogenic response of the adherent cells to different surface topographies was monitored by gene expression analysis.

2.1 Sample preparation

TNT arrays were prepared according to previous studies via an electrochemical anodization method.[20,21] Titanium (Ti) foils (99.7%, 0.25mm thick, Sigma-Aldrich, St. Louis, MO, USA) were cut into 1cm^2 and 4cm^2 squares to fit 24-well plates and 6-well plates (Corning, NY, USA) for cell culture, respectively. Prior to the anodization, the samples were polished to remove the natural oxide layer using 600 and 1200 grit silicon carbide abrasive paper disks and sonicated with acetone, 70% ethanol and distilled water sequentially for 15min each. After cleaning, the air-dried Ti samples were connected to an electrochemical reaction flask having a two-electrode configuration: a platinum foil (Alfa Aesa, Ward Hill, MA, USA) cathode and the Ti anode. The cathode and anode were connected to a DC power supply. In order to create nanotubes on Ti surface, 10 or 30 volts were applied and nanotubes were generated in a glycerol based electrolyte with 0.25 wt % ammonium fluoride (96%, Alfa Aesar, Ward Hill, MA, USA) and 2 vol% deionized water. The anodized samples were then washed with deionized water, dried at 80°C and heat-treated at 500°C with a muffle furnace (Thermolyne 6000, Waltham, MA USA) for 3 h to transform amorphous titanium oxide (TiO2) nanotubes to crystalline anatase. The samples used for all experiments were sterilized with 70% ethanol and UV light overnight prior to use. The polished and non-anodized Ti plates were used as the control (Flat Ti). The Flat Ti was cleaned, dried and sterilized with the same process as the experimental samples (TNTs made of 10v and 30v voltage).

2.2 Cell culture

To observe the effects of TNTs on cell behaviour, MC3T3-E1 mouse preosteoblasts (ATCC, Washington, DC) were cultured in regular medium: alpha-minimum essential medium (αMEM) with 10% fetal bovine serum and 1% penicillin / streptomycin (PS) under 37°C, 5% CO_2 environment. Cells were seeded onto the control and experimental substrates that were placed within polystyrene culture plates. The culture media was changed every 3 days. In order to investigate if FAK and RhoA play a role in cell growth, 500nM PF573228 (Sigma-Aldrich, St. Louis, MO, USA) and 200ng/ml C3 (Cytoskeleton, Hoboken, NJ, USA) were respectively[22,23] used to inhibit FAK phosphorylation at Y397 and RhoA activity. 10μM Rock inhibitor Y27632 [24] was also applied to confirm the role of RhoA on cell proliferation.

2.3 Scanning electron microscopy observation

Surface characterization of the specimens and the adhered MC3T3-E1 cells were conducted with SEM (Hitachi S-4700 Cold Cathode Field Emission Scanning Electron Microscope, Tokyo, Japan). A 10 kV accelerating voltage was chosen for SEM analysis and the secondary electrons were captured with an in-lens detector, and surfaces were rendered at magnification of 30,000 and 50,000.

2.4 Cell cycle analysis

Based on the BrdU result of MC3T3-E1 cells cultured on three substrates with regular media, the analysis of cell cycle during early culture stage was performed with FACS. MC3T3-E1 cells (2.5×10^4/ml) were placed on each of the three substrates for 24 hours (n=2). After incubation, the cells were trypsinized and washed with ice-cold PBS, centrifuged at 2000 rpm for 5 min and fixed with 2.5 mL 70% ice-cold ethanol at 4°C for 24 h. Cells were washed again after fixation, and resuspended in 500 μL PBS solution containing 0.05 mg/mL propidium iodide (PI) and 0.2 mg/mL RNAse, and then incubated at 4°C for 2 h. Fluorescence was measured with a FACSCanII flow cytometer, using PE ×FL2 channels. The assay was carried out in three independent experiments and 10,000 events were analyzed per experiment using the FlowJo software.

2.5 BrdU Cell proliferation Assay

The BrdU assay was carried out to test the proliferation level of the cells cultured with the regular medium (control group) and the condition medium respectively contained FAK inhibitor and RhoA activity inhibitor. Cells (2.5×10^4/ml) were seeded on 1cm × 1cm Flat Ti and TNTs samples, which were placed in 24-well plates. At Day 1 and 7, cells were treated with BrdU (BD Biociences, San Jose, US) for 2 hours and then fixed with 4% formaldehyde (Tousimis®, Rockville, US) for 1h. The samples were then incubated with monoclonal mouse anti-BrdU primary antibody at 4°C overnight, followed by biotinylated goat anti-mouse IgG (H+L) secondary antibody (Invitrogen, Carlsbad, CA, USA) for 60min and DAPI for 15min. The proliferation level was indicated by the ratio of BrdU labeled cell to the adhered cell (DAPI) on each sample (n=6). All cells were visualized using a Nikon fluorescence microscope with TRITC and DAPI filters, and a Nikon Eclipse Ti-U digital camera (Nikon Instruments, Melville, NY). Nikon NIS Elements software was used to

acquire the fluorescent merged image and the images were processed and analyzed with Image J.

2.6 Cell morphology

To detect the morphology change of MC3T3-E1 cells on different substrates, Focal Adhesion Staining Assay was applied to the cells cultured with regular media. Cells (2.5×10^3/ml) were seeded on 1cm × 1cm Flat Ti and TNTs samples placed in 24-well plates. At the end of the 12h culture, the cells were first fixed in 4% formaldehyde for 15 min, then permeabilized with 0.1% Triton X100 (Sigma-Aldrich, St. Louis, MO, USA) for 15 min followed by blocking in 1% bovine serum albumin (Gibco, Gran Island, NY, USA) for 30min. Primary antibody incubation was carried out at 4°C overnight, while vinculin, F-actin and nuclear were counterstained, respectively, for 1h and 15min with Actin Cytoskeleton and Focal Adhesion Staining Kit (Millipore, Billerica, MA, USA). Both primary and secondary antibodies were diluted in 1% bovine serum in phosphate buffered saline (PBS). The vinculin, F-actin phalloidin and DAPI stains were observed with a Nikon fluorescence microscope with TRITC, FITC and DAPI filters. All the images were acquired with a Nikon Eclipse Ti-U digital camera (Nikon Instruments, Melville, NY) and the merged fluorescent images were acquired and analyzed by Nikon NIS Elements software. More than 80 cells on each sample were measured (n=6). The length to width aspect ratio was used to indicate the elongation of the cell, and the area of single cell spreading was obtained with an automatic optical threshold defined by the software. The cell elongation and area were compared among different tube diameters.

2.7 Protein isolation and Western Blot analysis

The expression of FAK, RhoA, phosphorylated FAK, was examined with Western Blot analysis. Cells (2.5×10^4 cell/ml) with 2ml growth medium were cultured per well on 2cm×2cm flat Ti and TNTs samples placed in 6-well plates 24h prior to harvest. Cells were lysed in 1×RIPA buffer (Cell Signaling, Danvers, MA, USA) with protease and phosphatase inhibitors (Sigma-Aldrich, St. Louis, MO, USA). The supernatant collected after centrifuging for 15 min at 14,000 rpm and 4°C. Protein concentration of cell lysate was detected by using the Bradford method with Pierce® BCA Protein Assay Kit (Thermo Scientific, Tewksbury, MA, USA). The protein concentration was equalized by diluting with lysis buffer, and then all cell lysates were fractionated by electrophoresis in 10% polyacrylamide gels and electrotransferred to polyvinylidene difluoride (PVDF) film. After blocking with 5% w/v bovine serum albumin (BSA) solution in TBS-T (10mM Tris, 150mM NaCl, 0.05% v/v Tween 20), the blots were exposed to rabbit antibodies specific to mouse FAK (Cell Signaling, Danvers, MA, USA), phosphorylated FAK (pY397) (Cell Signaling, Danvers, MA, USA) and RhoA (Sigma-Aldrich, St. Louis, MO, USA). After reacting with secondary antibodies (Vector Laboratories, UK), immunoreactive bands were visualized using enhanced chemiluminescence detection and quantified using densitometry analysis with Imagequant LAS4000 software (GE Healthcare, Cleveland, Ohio, USA). The ratio of RhoA/FAK expression was calculated from densitometric values. Blots were stripped and reprobed for the loading control of GAPDH (Cell Signaling, Danvers, MA, USA). Immunoblots were carried out from four independent individual experiments (n=4).

The mean and standard deviation of GAPDH-normalized intensities were calculated with Image J.

2.8 Measurement of RhoA activity

RhoA activity was examined with G-LISA™ RhoA activation assay kit (Cytoskeleton, Inc., Denver, CO). According to the manufacturer's instructions, the cell lysates were obtained from MC3T3-E1 cells cultured on three substrates and the protein concentration was equalized to 1.5 mg/ml for assay. The cell extracts were transferred into a 96-well plate which was coated with Rho-GTP binding protein. The inactive GDP-bound Rho was removed afterwards through the washing steps. A specific RhoA antibody and an HRP-conjugated secondary antibody were applied to detect the bound active RhoA and the luminescence was read on microplate reader (Molecular Devices LLC, Sunnyvale, CA, USA).

2.9 Quantitative real-time PCR

According to the cell proliferation result at late culture stage, the osteogenic gene markers were detected to test whether there was an alteration of cell fate. Cells (2.5×10^4/ml) were seeded on 2cm × 2cm flat Ti and TNTs samples, which were placed in 6-well plates. The expression levels of osteogenesis related genes were measured using the quantitative reverse transcription polymerase chain reaction (qRT-PCR). RNA was extracted using TRIzol® Reagent (Invitrogen, Carlsbad, CA, USA) at days 4, 7, 14, and 21 after seeding. An equivalent amount of RNA from each sample was reverse transcribed into complementary DNA (cDNA) using the iScript™ cDNA Synthesis Kit (Bio-Rad Laboratories, Hercules, CA, USA). The qRT-PCR analysis of genes including Runt-related transcription factor 2(Runx2), bone sialoprotein (BSP), Osterix (Osx) and osteocalcin (OCN) were performed on the Applied Biosystems 7500 (Applied Biosystems, Foster City, CA, USA) using the Taq DNA Polymerase (Invitrogen, Carlsbad, CA, USA). Specific primers were used for each target gene (Table 1). The expression levels of the target genes were normalized to that of the housekeeping gene GAPDH (n=4).

2.10 Statistical analysis

Numerical data were analyzed with Multi-factorial Analysis of Variance and a non-linear regression of different protein expressions (BrdU = $\alpha 0$ + $\alpha 1$ FAK + $\alpha 2$ RhoA + $\alpha 3$ RhoA/FAK) was used to predict factors influencing cell proliferation. Statistical difference was considered at $p < 0.05$. All experiments were completed three times with three replicates used for each experiment.

3. Results

3.1 Fabrication of titanium nanotubes and cell morphology

Nanotubes of different pore size were evenly distributed after anodization and annealing treatment and the robust and discrete shape of the nanotopology was confirmed by SEM images (Figure 1). Nanotubes of 40nm and 150 nm diameters were found after 3h anodization with 10v and 30v voltage (Figure 1B, 1C), respectively, while the control titanium foil (Flat Ti) showed no nanotopography (Figure 1A). The TNTs made using 10v

and 30v were not highly ordered or aligned. MC3T3 cells cultured on the control titanium foil showed wide spreading and more flat morphology and less noticeable filopodia (Figure 1D). On the contrary, cells on the 40nm and 150nm nanotubes showed greater spatial shape with filopodia and lamellipodia extensions (Figure 1E & F) after 12h culture. The elongation of MC3T3 cells on 150nm diameter nanotubes was confirmed by immunofluorescent staining of vinculin and F-actin (Figure 2). On Flat Ti substrates, more visualized focal contacts (green vinculin-binding spots) were found distributed at the edge of the cells; less staining was observed in 40nm TNTs and the least staining was found on the 150nm TNTs (Figure 2A,2B). The adherent cells on larger TNTs exhibited extraordinary cellular protrusion whereas their spreading area presented significant reduction (Figure 2C). The elongation was more than twice as much as on the Flat Ti surface, and 1.5 times greater than that of the 40nm nanotube (Figure 2D). All observations in morphological changes assessed by SEM and staining were similar.

3.2 Cell cycle and proliferation

The BrdU assay and the cell cycle analysis were both performed to observe the change of cell proliferation level at early stage. Flow cytometric analysis demonstrated changes in cell cycle progression on three substrates (Figures 3A). As shown in Figure 3B, TNTs increased the number of cells in S-phases compared with Flat Ti (6.62%), and such elevated S-phase proportion was most obvious in 150nm TNTs (25.04%). Moreover, no significant increase was found in G2/M phase for the cells grown on TNTs.

Figure 4A showed the images of BrdU immunofluorescence staining for the cells cultured on Day 1. The average number of BrdU labeled cell to total adhered cell on Flat Ti, 40nm TNTs and 150nm TNTs were respectively 17.06%, 18.58% and 28.6% within 24h (Figure 4B). However this ratio dropped down to 16.78%, 14.41% and 11.61% after 7days culture. Although the cell growth was repressed at both time points and for all three substrates after the FAK Y397 phosphorylation was inhibited, the cells on 150nm TNTs still presented higher proliferation level (20.17%) during the first 24 hours.

The cells treated with C3 showed greatest reduced proliferation rate in all groups at 1 and 7 days but with the most remarkable declination being found in 150nm TNTs group (Figure 4). When C3 and PF573228 were both applied, the cell growth was inhibited in TNTs groups, which were not only reflected by cell count of BrdU staining but also confirmed by fluorescent intensity. Relatively speaking, C3+ and C3+ PF573228 group appeared to have almost the same low level of cell growth except for the control condition at day one. To detect the effects of ROCK inhibitor on cell proliferation, we further treated the cells with Y27632 for 24 hours in all groups. As shown in Figure S1, the cell growth also appeared significant declination, especially in 150nm TNTs group.

3.3 FAK, pY397-FAK, RhoA Protein Expression and RhoA activity

Based on the Focal Adhesion Staining and proliferation result, the expression of FAK and RhoA on TNTs were compared with that on Flat Ti. Western blot result of total FAK, phosphorylated FAK (pY397-FAK), RhoA and GAPDH showed prominent difference after 1 day culture (Figure 5A). FAK protein expression in 40nm and 150nm TNTs group were

respectively 50.1% and 86.2% less than Flat Ti group (Figure 5B). Meanwhile, the pY397-FAK expressed at a lower level on TNTs as well (Figure 5C), which was consistent with that of total FAK expression. The cells cultured on TNTs performed significantly decreased RhoA activity as shown in Figure 5D, though the difference between 40nm and 150nm TNTs was not obvious. Activation of RhoA in larger TNTs group declined to 63.12 ± 1.5% compared with on Flat Ti. On 150nm TNTs, while the protein level of RhoA also decreased (Figure 5E), the relative expression of RhoA compared with FAK was found significantly higher (Figure 5F). The densitometry analysis of the RhoA/FAK ratio: 1.38 on Flat Ti, 1.22 on 40nm TNTs and 3.08 on 150nm TNTs. The non-linear regression analysis showed that RhoA/FAK ratio was the most significant factor ($p=0.0017$) relating to cell proliferation. FAK or RhoA alone was not related to proliferation ($p>0.05$) (Table 2).

3.4 Osteogenic gene expressions

The osteodifferentiation of the cells on three substrates was detected at the late culture stage. Runx2, BSP, Osx and OCN were assessed by the qRT-PCR and the expression of all these osteogenesis markers showed significant difference over time (Figure 6). TNTs of different diameter triggered higher gene levels compared with Flat Ti. Generally, 150nm TNTs induced the highest mRNA expression for all these osteogenic genes.

4. Discussion

A prominent effect of altered substrate nanotopography is reflected by the change of cell morphology, and recent studies also presented the similar result.[2,6,25] Compared with the 40nm TNTs, the 150nm TNTs promoted the adherent cells to be less spread and have a more elongated morphology. Topography-induced cellular behavior is aroused by a mechanical force transducer-focal adhesions (FAs),[26] through which the geometric inputs from ECM are delivered and translated into the formation of intracellular cytoskeleton. One key event in FA assembly is the focal adhesion kinase (FAK) which act as signaling “hubs” in FA complex network. The physical structure of ECM and cell/biomaterial interaction regulate the phosphorylation of FAK at Y397. Since the visualized focal contacts were diminished on 150nm TNTs, we hypothesized that the FAK or phosphorylated FAK expression is impaired by nanotopography due to the reduction of total contact surface available. Our result of western blot showed a significant reduction in the expression of total FAK as well as pY397-FAK, which were consistent with earlier studies using TCPS or PLLA for a different nanoscale of gratings and pits.[27,28]

Further influence of topography was observed at the level of proliferation. Increased cell proliferation was observed at early stages in culture among cells adherent to 150nm TNTs as corroborated by Flow cytometry analysis and BrdU immunochemistry staining. The increased proportion of S phase as well as the absence of G2/M phase accumulation illustrated higher proliferation level in these cells. It is likely that the alterations in FA number and / or FAK phosphorylation that occurred as a function of TNT dimension plays a key role in regulating proliferation.

Changing TNT diameter led to coordinated, inverse changes in measured cell proliferation. Concurrently, reduced numbers of Focal contacts and FAK expression was observed. While

FAK plays a prominent part in regulation of proliferation[13,14] and its phosphorylation status is related to topography induced cell behavior,[4] we further explored whether the reduced phosphorylated FAK (pY397-FAK) level led to the proliferation change on 150nm TNTs in both early and late stage of cell culture. When the pY397-FAK inhibitor was added to cultures, PF573228 down regulated cell proliferation on all the three substrates and time points, whereas on 150nm TNTs, proliferation remained at relatively higher levels (20.17%) during the first 24 hours. In this respect, it is tempting to speculate that the relatively high proliferation during the early stage on large TNTs was due to either the multifaceted function of FAK or other potential compensation signaling pathways.

RhoA has been suggested to play a compensatory role in providing a permissive condition for cell proliferation in FAK−/− cells whose adhesive condition is deficient[13]. The nanotubular topography impeded total FAK expression and the outcome might be analogous to the situation of FAK knock down. In this investigation, we explored the potential compensatory role of RhoA in regulation of cell proliferation where FAK stimulus was apparently reduced. However, using a pharmacological approach, Yang found that slightly decreased RhoA expression could increase proliferation in poorly adhering cells.[29] Our results that RhoA activity is inversely proportional to cell proliferation are also consistent with earlier studies.[30] The treatment of cells adherent to 150nm TNTs with the RhoA inhibitor effectively influenced proliferation, and the similar result was also observed when using ROCK inhibitor. While there are measureable reductions of FAK in cells adherent to both 40nm and 150 nm TNTs, only on 150 nm TNTs was the ratio of RhoA/FAK significantly altered (Figure 5E). The relatively greater influence of C3 versus PF573228 on proliferation suggests that the higher RhoA/FAK ratio may be important in resolving these multiple intracellular signals. Suggested is a specified role of the relative expression of RhoA compared with FAK, which can be regulated by substrates in a topography dependent manner, perhaps can be traced back to the topography-induced restrictions imposed by cell shape and cytoarchitecture.

In addition, to further investigate the complementary role of RhoA in FAK related cell growth, cells were treated with both PF573228 and C3. Cell proliferation was eliminated and pY397-FAK inhibition failed to rescue the cell growth. Multi-factorial Analysis of Variance confirmed that RhoA inhibition had more prominent negative effects than the blockage of FAK autophosphorylation. Our findings were consistent with the biological theorem demonstrated in an earlier study.[13]

Moreover, we also tested the osteodifferentiation capability of MC3T3-E1 cells cultured on TNTs substrates. Compared with flat Ti, the osteogenetic marker gene has been remarkably promoted 4 days after MC3T3 cells were cultured on 150nm TNTs. The process of osteogenic differentiation was solely induced by topographical cue, since no chemical treatment was adopted. These results were in agreement with earlier studies.[31–33] The proliferation and differentiation process of the cell do not occur simultaneously, and the cell functional maturation only happens after cell growth.[34] Therefore, the enhanced osteogenic cell fate and function could be the main reason for the declined proliferation level 3 days after seeding on bigger size TNTs. Our limited data, however, cannot directly prove the

promotion of mineralization by TNTs; future studies with mineralization assays may uncover the RhoA/FAK derived osteogenic effect.

Another limitation of the present study is the lack of investigation of the effects of TNTs density and orientation on cell behaviour and other integrin mediated pathways, such as Src, Ras, PI3K, and Rac. Because of FAK serves as the “hub” of intracellular mechanotransduction and RhoA works as an essential downstream factor of FAK, we, therefore, focus on the expression and function of FAK and RhoA in response to TNTs. Our outcome is to be carefully interpreted without considering other relative pathways.

Taken together, the nanotubular topography impeded the total FAK expression and the outcome might mimic the situation of FAK knocking down, in which process other compensatory factors, such as RhoA, may consequently rescue cell proliferation.

5. Conclusions

The TNTs had noticeable effects on MC3T3-E1 cells behavior, not only in cell morphology but also cell proliferation. In this study, we found that MC3T3-E1 cell proliferation can be affected by TNTs, and the promotion of cell growth at early stage triggered by such topographical factor are observed to be associated with RhoA and FAK. This phenomenon works more prominent for TNTs with larger diameter, and the relatively high RhoA/FAK ratio is proposed to contribute more to this observation than the impeded FAK expression. Future studies will delineate more about the mechanism of FAK and RhoA involvement, as well as the interaction of their activity in nanotopography regulated cell behavior, and provide a basis for manipulating and the use of nanostructure in artificial orthopedic implant.

Supplementary Material

Refer to Web version on PubMed Central for supplementary material.

Acknowledgments

This work was supported, in part, by NIH/NIDCR R01DE022816-01 and the North Carolina Biotech Center. The work was also supported by Chongqing Natural Science Foundation (CSTC2012jjA10106), the Specialized Research Fund for the D octoral Program of China (SRFDP20125503120009), Chongqing Municipal Health Bureau (2012-2-121), Project Supported by Program for Innovation Team Building at Institutions of Higher Education in Chongqing in 2013, and a Project Supported by Chongqing Municipal Key Laboratory of Oral Biomedical Engineering of Higher Education.

Notes and references

1. Pignatello R. Biomaterials Science and Engineering. 2011
2. Oh S, Brammer KS, Li YS, Teng D, Engler AJ, Chien S, Jin S. Proceedings of the National Academy of Sciences of the United States of America. 2009; 106:2130–2135. [PubMed: 19179282]
3. Yang S, Wang M, Zhang H, Cai K-y, Shen X-k, Deng F, Zhang Y, Wang L. RSC Advances. 2014; 4:65163–65172.
4. Teo BK, Wong ST, Lim CK, Kung TY, Yap CH, Ramagopal Y, Romer LH, Yim EK. ACS Nano. 2013; 7:4785–4798. [PubMed: 23672596]

5. Minagar S, Wang J, Berndt CC, Ivanova EP, Wen C. Journal of biomedical materials research Part A. 2013; 101:2726–2739. [PubMed: 23436766]
6. Brammer KS, Oh S, Cobb CJ, Bjursten LM, van der Heyde H, Jin S. Acta biomaterialia. 2009; 5:3215–3223. [PubMed: 19447210]
7. Wang N, Li H, Lu W, Li J, Wang J, Zhang Z, Liu Y. Biomaterials. 2011; 32:6900–6911. [PubMed: 21733571]
8. Anselme K, Davidson P, Popa AM, Giazzon M, Liley M, Ploux L. Acta biomaterialia. 2010; 6:3824–3846. [PubMed: 20371386]
9. Schlaepfer HCDD, Sieg DJ. Progress in biophysics and molecular biology. 1999; 71:435–478. [PubMed: 10354709]
10. Ross TD, Coon BG, Yun S, Baeyens N, Tanaka K, Ouyang M, Schwartz MA. Current opinion in cell biology. 2013; 25:613–618. [PubMed: 23797029]
11. Parsons JT. Journal of cell science. 2003; 116:1409–1416. [PubMed: 12640026]
12. Wozniak MA, Chen CS. Nature reviews Molecular cell biology. 2009; 10:34–43.
13. Pirone DM, Liu WF, Ruiz SA, Gao L, Raghavan S, Lemmon CA, Romer LH, Chen CS. The Journal of cell biology. 2006; 174:277–288. [PubMed: 16847103]
14. Kaneda T, Sonoda Y, Ando K, Suzuki T, Sasaki Y, Oshio T, Tago M, Kasahara T. Cancer letters. 2008; 270:354–361. [PubMed: 18606490]
15. Zhao JH, Reiske H, Guan JL. The Journal of cell biology. 1998; 143:1997–2008. [PubMed: 9864370]
16. Duxbury MS, Ito H, Benoit E, Zinner MJ, Ashley SW, Whang EE. Biochemical and biophysical research communications. 2003; 311:786–792. [PubMed: 14623342]
17. WGK; Clark, Edwin A.; Brugge, Joan S.; Symons, Marc; Hynes, Richard O. The Journal of cell biology. 1998
18. Mammoto A, Huang S, Moore K, Oh P, Ingber DE. The Journal of biological chemistry. 2004; 279:26323–26330. [PubMed: 15096506]
19. Olson MF, Paterson HF, Marshall CJ. Nature. 1998; 394:295–299. [PubMed: 9685162]
20. Hu Y, Cai K, Luo Z, Xu D, Xie D, Huang Y, Yang W, Liu P. Acta biomaterialia. 2012; 8:439–448. [PubMed: 22040682]
21. Macak JM, Hildebrand H, Marten-Jahns U, Schmuki P. Journal of Electroanalytical Chemistry. 2008; 621:254–266.
22. Courter D, Cao H, Kwok S, Kong C, Banh A, Kuo P, Bouley DM, Vice C, Brustugun OT, Denko NC, Koong AC, Giaccia A, Le QT. PloS one. 2010; 5:e9633. [PubMed: 20224789]
23. Heusinger-Ribeiro J, Eberlein M, Wahab NA, Goppelt-Struebe M. Journal of the American Society of Nephrology : JASN. 2001; 12:1853–1861. [PubMed: 11518778]
24. Xu Y, Wagner DR, Bekerman E, Chiou M, James AW, Carter D, Longaker MT. PloS one. 2010; 5:e11279. [PubMed: 20585662]
25. Park J, Bauer S, von der Mark K, Schmuki P. Nano letters. 2007; 7:1686–1691. [PubMed: 17503870]
26. Frey MT, Tsai IY, Russell TP, Hanks SK, Wang YL. Biophysical journal. 2006; 90:3774–3782. [PubMed: 16500965]
27. Lim JY, Dreiss AD, Zhou Z, Hansen JC, Siedlecki CA, Hengstebeck RW, Cheng J, Winograd N, Donahue HJ. Biomaterials. 2007; 28:1787–1797. [PubMed: 17218005]
28. Yim EK, Darling EM, Kulangara K, Guilak F, Leong KW. Biomaterials. 2010; 31:1299–1306. [PubMed: 19879643]
29. Yang X, Zheng F, Zhang S, Lu J. Biomedicine & pharmacotherapy = Biomedecine & pharmacotherapie. 2015; 69:361–366. [PubMed: 25661383]
30. Yang S, Kim HM. Biomaterials. 2012; 33:2902–2915. [PubMed: 22244698]
31. Popat KC, Leoni L, Grimes CA, Desai TA. Biomaterials. 2007; 28:3188–3197. [PubMed: 17449092]
32. Woo KM, Jun JH, Chen VJ, Seo J, Baek JH, Ryoo HM, Kim GS, Somerman MJ, Ma PX. Biomaterials. 2007; 28:335–343. [PubMed: 16854461]

33. Cha KJ, Hong JM, Cho DW, Kim DS. Biofabrication. 2013; 5:025007. [PubMed: 23548407]
34. Birmingham EN, GL, McHugh PE. European Cells and Materials. 2012; 23:13–27. [PubMed: 22241610]

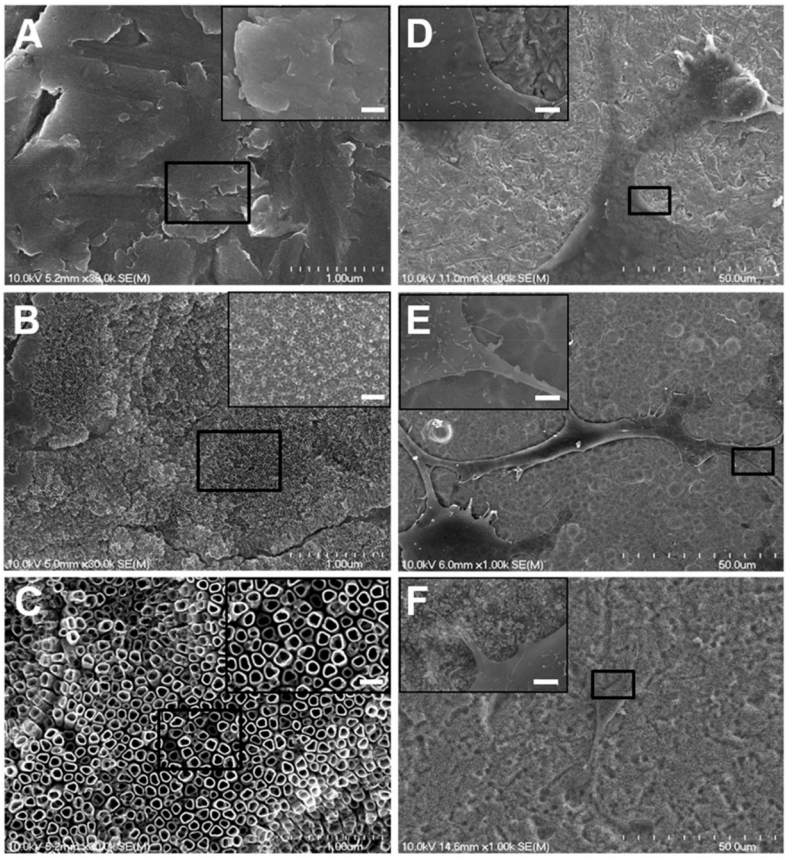

Fig. 1.

Scanning electron microscopy (SEM) observation of TNTs morphology and MC3T3-E1 cells attachment. (A) Flat Ti, (B) 40nm TNTs and (C) 150nm TNTs. Adherent MC3T3-E1 cells on Flat Ti (D), 40nm TNTs (E) and 150nm TNTs (F). For enlarged sections the scale bars equals 0.2 μm.

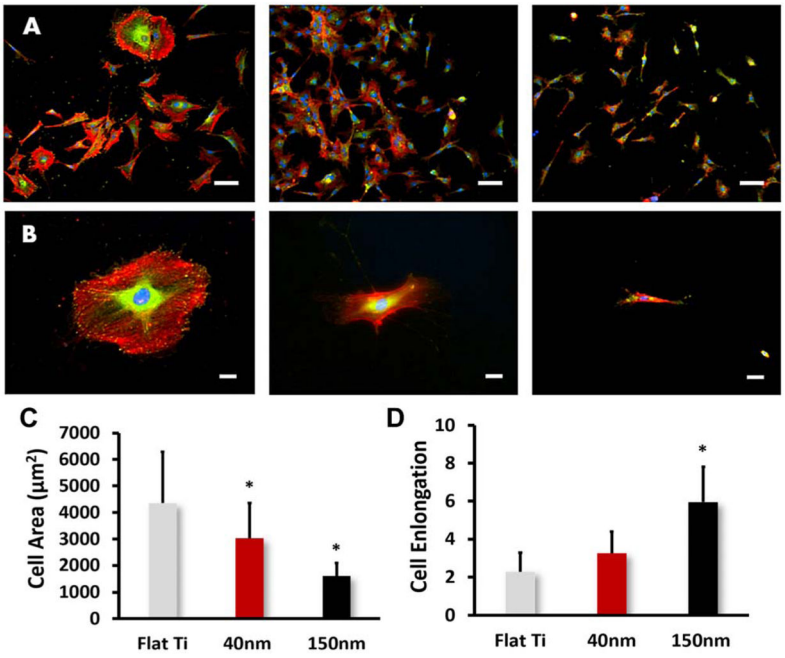

Fig. 2.

Immunofluorescent images of vinculin (FITC-green), cytoskeletal actin (TRITC-red) and nucleus-staining (DAPI-blue) for MC3T3 cells on Flat Ti, 40nm TNTs and 120nm TNTs. (A) Magnification of 10× (Scale bars = 200 μm), (B) Magnification of 20× (Scale bars = 50 μm), (C) Cell area and elongation vs. nanotube size. The bar graphs show the average ± standard error bars. Statistical significance ($p < 0.05$) are marked on the graphs with *.

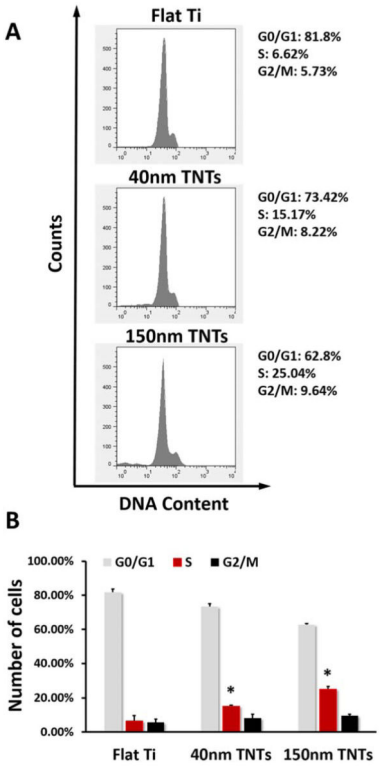

Fig. 3.

(A) Flow cytometry analysis of MC3T3-E1 cell cycle on different substrates after 24h culture, (B) Percentage of MC3T3-E1 cells in G1, S and G2 phases on different substrates. The statistical significance ($p < 0.05$) after performing t-tests are marked: *, indicates a significant difference between the same phase of the cells growing on different substrates, compared with Flat Ti.

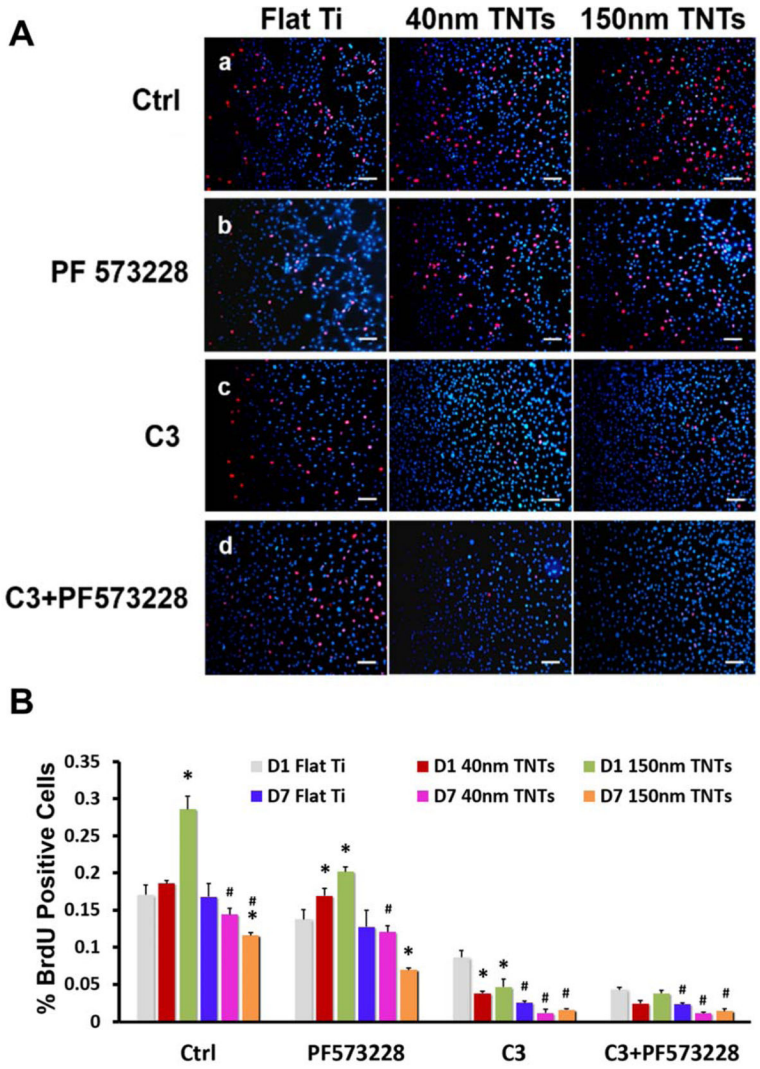

Fig. 4.

(A) Immunofluorescent images of BrdU-labeled nuclei (imerged image of TRITC-red and DAPI-blue) for MC3T3-E1 cells after one day culture. Scale bars = 200 μm. a. control group (regular medium), b. Regular medium + PF573228, c. Regular medium + C3 and d. Regular medium+ C3 + PF573228. (B) Quantification of BrdU-labeled nuclei for Day 1 and Day 7 culture. The statistical significance ($p < 0.05$) after performing t-tests are marked: *, indicates a significant difference between the cells growing on different substrates with same treatment and at the same time point, compared with Flat Ti; #, denotes a significant difference between different time points on the same substrate and with same treatment, compare with D1.

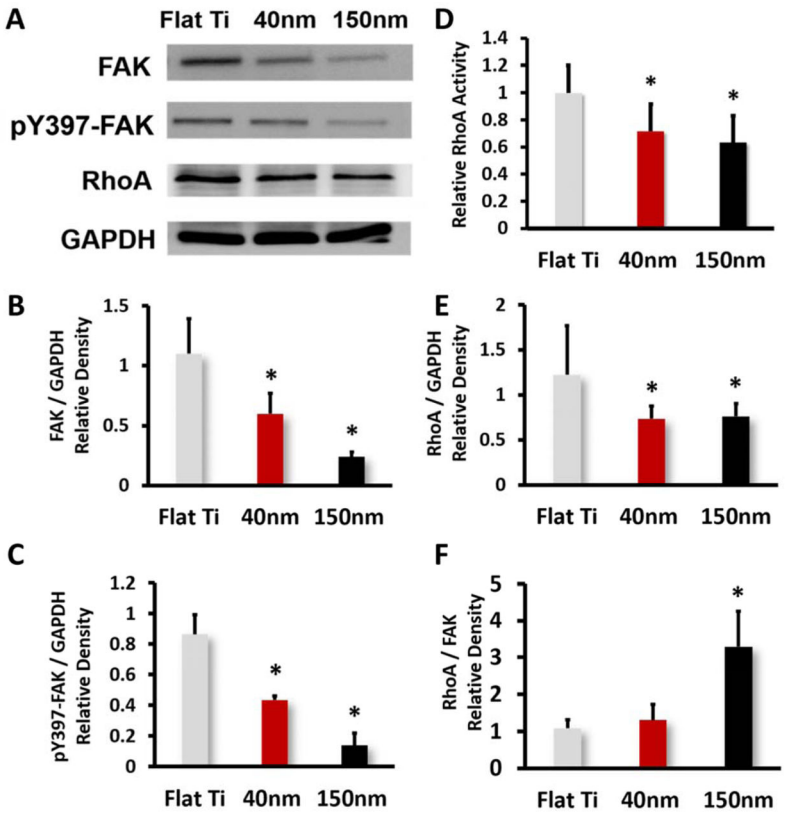

Fig. 5.

(A) Protein expression level of FAK, pY397-FAK and RhoA in MC3T3-E1 cells after one day culture on different substrates, (B) Densitometric quantification of total FAK, (C) Densitometric quantification of pY397-FAK, (D) RhoA activity level detected with G-LISA™ assay, (E) Densitometric quantification of RhoA and (F) Densitometric quantification of RhoA/FAK. Values are expressed as means ± SD. * Significant difference in protein expression of cells on different substrats ($p < 0.05$).

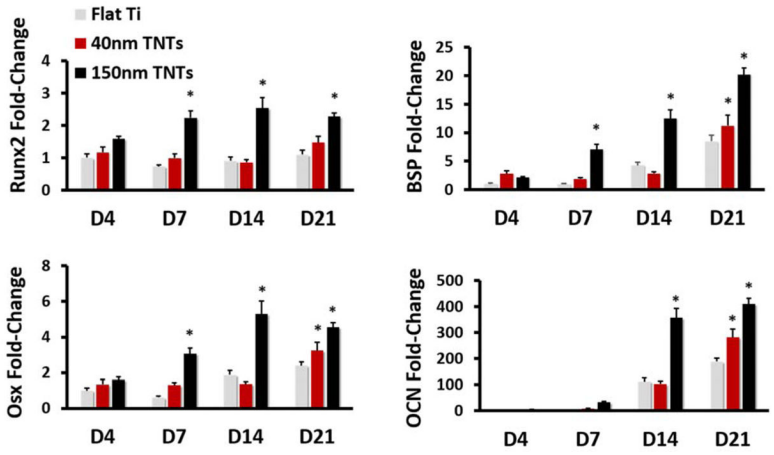

Fig. 6.

Gene expression of osteoblast markers in MC3T3-E1 cells after 4, 7, 14 and 21 days of culture. Fold change of Runx2, BSP, Osx and OCN ($p < 0.05$). * indicates a significant difference between different substrates.

Table 1

qRT-PCR Primers.

Gene	Forward primer sequence(5′-3′)	Reverse primer sequence(5′-3′)
BSP	CCGGCCACGCTACTTTCTT	TGGACTGAAACCGTTTCAGA
Runx2	GAATGGCAGCACGCTATTAAATCC	GCCGCTAGAATTCAAAACAGTTGG
Osx	CCTCTCGACCCGACTGCAGATC	AGCTGCAAGCTCTCTGTAACCATGAC
OCN	CTGACCTCACAGATGCCAA	GGTCTGATAGCTCGTCACAA
GAPDH	TGAGGTGACCGCATCTTCTTG	TGGTAACCAGGCGTCCGATA

Table 2

Parameter estimates of non-linear regression analysis.

Term	Estimate	Std Error	t Ratio	Prob>|t|
Intercept	0.1486073	0.037882	3.92	0.0044*
FAK	0.0230961	0.06212	0.37	0.7197
RhoA	−0.046325	0.037728	−1.23	0.2544
RhoA/FAK	0.0508234	0.015633	3.25	0.0117*

*Significant difference $P < 0.05$.